Copy
RM E53L23

NACA

RESEARCH MEMORANDUM

THRUST CHARACTERISTICS OF A SERIES OF CONVERGENT-DIVERGENT

EXHAUST NOZZLES AT SUBSONIC AND SUPERSONIC FLIGHT SPEEDS

By Evan A. Fradenburgh, Gerald C. Gorton, and Andrew Beke

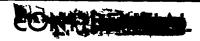Lewis Flight Propulsion Laboratory
Cleveland, Ohio

CLASSIFIED DOCUMENT

NATIONAL ADVISORY COMMITTEE
FOR AERONAUTICS
WASHINGTON
March 12, 1954

NACA RM E53L23   CONFIDENTIAL

3142

CP-1

NATIONAL ADVISORY COMMITTEE FOR AERONAUTICS

RESEARCH MEMORANDUM

THRUST CHARACTERISTICS OF A SERIES OF CONVERGENT-DIVERGENT EXHAUST

NOZZLES AT SUBSONIC AND SUPERSONIC FLIGHT SPEEDS

By Evan A. Fradenburgh, Gerald C. Gorton, and Andrew Beke

SUMMARY

An experimental investigation of a series of four convergent-divergent exhaust nozzles was conducted in the Lewis 8- by 6-foot supersonic wind tunnel at Mach numbers of 0.1, 0.6, 1.6, and 2.0 over a range of nozzle pressure ratios. The thrust characteristics of these nozzles were determined by a pressure-integration technique.
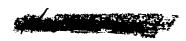
From a thrust standpoint, a nozzle designed to give uniform parallel flow at the exit had no advantage over the simple geometric design with conical convergent and divergent sections. The rapid-divergent nozzles might be competitive with the more gradual-divergent nozzles since the relatively short length of these nozzles would be advantageous from a weight standpoint and might result in smaller thrust losses due to friction.

The thrusts, with friction losses neglected, were predicted satisfactorily by one-dimensional theory for the nozzles with relatively gradual divergence. The thrusts of the rapid-divergent designs were several percentages below the theoretical values at the design pressure ratio or above, while at low pressure ratios there was a considerable effect of free-stream Mach number, with thrusts considerably above theoretical values at subsonic speeds and somewhat above theoretical values at supersonic speeds. This Mach number effect appeared to be related to the variation of the model base pressure with free-stream Mach number.

INTRODUCTION

As part of a general program on jet-engine-exit configurations being conducted in the Lewis 8- by 6-foot supersonic wind tunnel, a series of four convergent-divergent exhaust nozzles was investigated to determine the effects of nozzle contour on internal thrust characteristics. As previous experimental studies of nozzle performance have been largely limited to quiescent-air tests (ref. 1, e.g.), one of the main purposes

of the investigation was to examine any effect on jet thrust of the interaction between the exhaust jet and the external flow about the body housing the nozzle. The investigation is being continued to determine the effects of nozzle pressure ratio on external body drag and base drag for a convergent nozzle and for two of the convergent-divergent nozzles discussed herein. Thrust and external-body drag data for a plug-type nozzle are presented in reference 2.

In this report are discussed the internal pressure distributions and thrust characteristics of four convergent-divergent nozzles over a wide range of nozzle pressure ratios and at free-stream Mach numbers of 0.1, 0.6, 1.6, and 2.0.

SYMBOLS

The following symbols are used in this report:

A   internal flow area, sq ft

a   speed of sound, ft/sec

C_F thrust coefficient, F/P_1A_t

C_f nozzle mass-flow coefficient, m/m_1

F   nozzle jet thrust, $mV_e + A_e(p_e - p_0)$, lb

f/a   fuel-air ratio

g   acceleration due to gravity, 32.2 ft/sec^2

M   Mach number, V/a

m   mass flow, slug/sec

P   total pressure, $p\left(1 + \frac{\gamma - 1}{2} M^2\right)^{\frac{\gamma}{\gamma-1}}$, lb/sq ft

p   static pressure, lb/sq ft

R   gas constant for air, 53.3 ft-lb/(lb)(^{O}R)

r   body radius, in.

r_n nozzle internal radius, in.

V   velocity, ft/sec

x   distance from model nose, in.

α   model angle of attack, deg

γ   ratio of specific heats (1.4 used for calculations)

Subscripts:

a   beginning of afterbody

e   nozzle exit

i   ideal

s   sonic

t   nozzle throat

O   free stream

1   nozzle entrance

<div style="text-align:center">APPARATUS</div>

The equipment used in the jet-exit investigations is represented schematically in figure 1. Air from a high-pressure central laboratory supply was throttled by the control valve down to any desired operating pressure and preheated to approximately 400° F to avoid condensation effects in the nozzle. The air was introduced into the model through the two supporting struts of 18-inch chord and 11-percent-thick double-circular-arc airfoil section. The flexible piping external to the tunnel test section permitted rotation of the model about the support-strut center line to angles of attack of 8°. The air flow was measured by means of a standard A.S.M.E. sharp-edged orifice mounted ahead of the control valve, and the preheater fuel flow was measured with a rotameter.

Details of the model and the four nozzle configurations appear in figures 2 and 3; additional model details are given in reference 2. Instrumentation utilized in the present analysis included two equally spaced static-pressure orifices located approximately $2\frac{1}{2}$ inches ahead of the convergent section of the nozzle (station 1 in fig. 2) and three rows of static-pressure orifices in the divergent portion of each nozzle extending from the throat to the nozzle exit. There were seven orifices in each of the top and bottom rows and four in a side row, as indicated in figure 3. In addition, base pressures were measured by means of static-pressure orifices located between the inner and outer shells of the model.

Nozzle 1 was of simple geometric design, consisting of conical convergent and divergent sections faired together by a circular-arc section at the throat. This nozzle was geometrically similar to one tested in quiescent air and reported in reference 1. The ratio of the exit area to the throat area was 1.39, corresponding to a design nozzle pressure ratio (ratio of nozzle total pressure to free-stream static pressure) of 5.3.

Nozzle 2 was a uniform-exit configuration, designed by means of an axially symmetric characteristics diagram to produce a uniform, parallel exit flow of Mach number 1.8. The ratio of the exit area to the throat area was 1.43 and the design pressure ratio was 5.7. A relatively long convergent section was used to ensure reasonably uniform flow at the throat.

Nozzle 3 had the same area ratio and design pressure ratio as nozzle 2 and the same convergent section, but it had a rapid divergence to the exit diameter with a consequent reduction in over-all length. The area distribution in the divergent section corresponded to a constant Mach number gradient of 0.4 per inch if one-dimensional isentropic flow were assumed.

Nozzle 4 was also a rapid-divergent design identical with nozzle 3 except that it was extended to a larger exit diameter. The ratio of the exit area to the throat area was 1.83 for this nozzle, corresponding to a design pressure ratio of 9.1 based on one-dimensional flow.

Method of Calculation

An attempt was made to measure nozzle thrusts by the method reported in reference 2, which consists of determining model external drag and model thrust-minus-drag with two different mechanical arrangements by utilizing strain-gage balance measurements with corrections for several tare forces. The accumulated errors in this method were too large to be acceptable in the present investigation; therefore, a pressure-integration technique was used as an alternative.

The thrust was assumed to be composed of two parts: the theoretical "sonic thrust" at the throat of the nozzle, and the pressure-area contributions of the divergent section of the nozzle. The sonic thrust is equal to the total momentum parameter at the throat:

$$F_s = mV_t + (p_t - p_0)A_t = \gamma p_t M_t^2 A_t + (p_t - p_0)A_t \qquad (1)$$

With the assumptions of isentropic one-dimensional flow from the nozzle-entrance station and a Mach number of 1.0 at the throat,

$$F_s = \gamma P_1 \left(\frac{p}{P}\right)_{M=1} A_t + P_1 \left[\left(\frac{p}{P}\right)_{M=1} - \frac{p_0}{P_1}\right] A_t \tag{2}$$

A convenient thrust-coefficient definition for this analysis is thrust divided by nozzle total pressure and throat area. By this definition, the sonic-thrust coefficient is

$$C_{F,s} = \frac{F_s}{P_1 A_t} = \gamma \left(\frac{p}{P}\right)_{M=1} + \left(\frac{p}{P}\right)_{M=1} - \frac{p_0}{P_1} \tag{3}$$

For $\gamma = 1.4$, this sonic-thrust coefficient becomes

$$C_{F,s} = 1.268 - \frac{p_0}{P_1} \tag{4}$$

The thrust increment due to the divergent portion of the nozzle is equal to the integration of static pressure minus free-stream static pressure on the projected surface area. Thus,

$$\Delta F = \int_{A_t}^{A_e} (p - p_0)\, dA = P_1 A_t \int_1^{A_e/A_t} \frac{p}{P_1}\frac{dA}{A_t} - P_1 A_t \frac{p_0}{P_1}\left(\frac{A_e - A_t}{A_t}\right) \tag{5}$$

The thrust-coefficient increment is therefore

$$\Delta C_F = \frac{\Delta F}{P_1 A_t} = \int_1^{A_e/A_t} \frac{p}{P_1}\frac{dA}{A_t} - \frac{p_0}{P_1}\left(\frac{A_e}{A_t} - 1\right) \tag{6}$$

The total nozzle throat coefficient for $\gamma = 1.4$, when all losses in the converging section of the nozzle and the friction drag downstream of the throat are neglected, is the sum of equations (4) and (6):

$$C_F = C_{F,s} + \Delta C_F = 1.268 + \int_1^{A_e/A_t} \frac{p}{P_1}\frac{dA}{A_t} - \frac{p_0}{P_1}\frac{A_e}{A_t} \tag{7}$$

The thrust data presented herein are in a ratio form - thrust calculated by equation (7) divided by an "ideal" thrust. The ideal-thrust coefficient at any nozzle pressure ratio is defined as the isentropic one-dimensional value obtained when the nozzle geometry is such that the

exit pressure is equal to the free-stream static pressure. This thrust coefficient and the corresponding ideal exit-to-throat-area ratio are a function of the nozzle pressure ratio P_1/p_0 and the ratio of specific heats γ:

$$C_{F,i} = \frac{F_i}{P_1 A_t} = \frac{\gamma p_0 M_{e,i}^2 A_{e,i}}{P_1 A_t} \tag{8}$$

where

$$M_{e,i} = \sqrt{\frac{2}{\gamma - 1} \left[\left(\frac{P_1}{p_0} \right)^{\frac{\gamma-1}{\gamma}} - 1 \right]}$$

and

$$\frac{A_{e,i}}{A_t} = \frac{1}{M_{e,i}} \left[\frac{2 \left(1 + \frac{\gamma - 1}{2} M_{e,i}^2 \right)}{\gamma + 1} \right]^{\frac{\gamma+1}{2(\gamma-1)}}$$

Hence,

$$C_{F,i} = \gamma \sqrt{\frac{2}{\gamma - 1}} \left(\frac{2}{\gamma + 1} \right)^{\frac{\gamma+1}{2(\gamma-1)}} \sqrt{1 - \left(\frac{P_1}{p_0} \right)^{\frac{1-\gamma}{\gamma}}}$$

The nozzle mass-flow coefficient, defined as the ratio between the actual mass flow passing through the model and the ideal mass flow through the sonic throat of the nozzle, was calculated by means of the following equation:

$$C_f = \frac{m \left(1 + \frac{f}{a} \right)}{P_1 A_t \left(\frac{2}{\gamma + 1} \right)^{\frac{\gamma+1}{2(\gamma-1)}} \sqrt{\frac{\gamma}{gRT_1}}} \tag{9}$$

The nozzle total temperature T_1 was assumed to be the temperature measured at the entrance to the model. The nozzle total pressure P_1 was determined by the static-pressure measurements at the nozzle entrance

(station 1) and the Mach number at that station. This Mach number was computed according to continuity relations from the measured mass flow, static pressure, and total temperature.
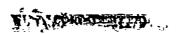
RESULTS AND DISCUSSION

The nozzle mass-flow coefficients for the four nozzles investigated are presented in figure 4. The data indicate values on the order of 0.99, with no appreciable effect of nozzle pressure ratio, free-stream Mach number, or angle of attack between zero and 8°.

Pressure distributions in the divergent portions of the four nozzles are presented in figures 5 to 8 as plots of the ratio of local static pressure to nozzle total pressure against the ratio of local to throat flow areas at free-stream Mach numbers of 0.1, 0.6, 1.6, and 2.0. The data presented are for zero angle of attack, but data obtained at an 8° angle of attack for the supersonic Mach numbers indicated no appreciable difference from those shown.

Each of the four nozzles had the characteristic that at the higher values of nozzle pressure ratio P_1/p_0 the pressure distribution curves were independent of both nozzle pressure ratio and free-stream Mach number. At the lower pressure ratios, usually considerably below design pressure ratio, the flow separated within the nozzle, resulting in significant increases in static pressure in the aft part of the divergent section. This latter effect was not, in general, independent of free-stream Mach number. As indicated by the constant values of throat pressure ratio, all nozzles apparently choked at the throat, even at the lowest nozzle pressure ratios.

The theoretical pressure distributions for isentropic one-dimensional flow are presented for all four nozzles in figures 5 to 8. The theoretical pressure distributions based on the method of characteristics are also shown for the uniform-exit and the rapid-divergent nozzle (figs. 6, 7, and 8). Nozzles 1 and 2, the conical-element and uniform-exit configurations, respectively, both have relatively long divergent sections; and the experimental pressure distributions for the higher nozzle pressure ratios agree reasonably well with one-dimensional theory, as might be expected. The data for nozzle 2 agree somewhat better with the theoretical distribution found by the method of characteristics, but for this nozzle the difference in the two theories is not large.

The experimental pressure distributions for the two rapid-divergent nozzles (figs. 7 and 8) fall substantially below the one-dimensional theory at the higher nozzle pressure ratios. Because of the high wall divergence angles on the divergent sections of these nozzles, it would

be expected that the Mach numbers near the wall would be higher than calculated by this theory. Characteristic diagrams for these nozzles indicated that the surface Mach number at the exit was approximately 2.1 for nozzle 3 and 2.5 for nozzle 4 compared with the one-dimensional values of 1.8 and 2.1, respectively. Corresponding to these higher Mach numbers, the surface static pressures would be less than the one-dimensional values at the design nozzle pressure ratio. The pressure distributions calculated from the characteristic diagrams were in much better agreement with the data.

Also presented in figures 5 to 8 are the experimental model base pressures obtained with the four nozzle configurations. The actual values of the base pressures have been divided by nozzle total pressures to make them comparable with the pressure-distribution data. For the case of unseparated flow at $M_0 > 1$, nozzles 1 and 2 with long diverging sections had base pressures below the nozzle-exit pressure; whereas the base pressures of nozzles 3 and 4, which were designed with more rapid divergence, were essentially the same or slightly higher than the nozzle-exit static pressure. No definite correlation between these pressures can be made since both are a function of afterbody design as well as nozzle design. For nozzles 3 and 4 below design pressure-ratio conditions, when the flow separated within the nozzle, the base pressure was always approximately equal to the exit pressure rather than the free-stream static pressure; for example, for nozzle 3 at a Mach number of 2.0 (fig. 7) the exit and base pressure ratios are approximately 0.35 for a nozzle pressure ratio of 1.90, whereas the free-stream pressure ratio p_0/P_1 is equal to 1/1.90 or 0.526. This was true for the nozzles of gradual divergence only at the lowest pressure ratios. The thrust for a given nozzle with separated flow is uniquely related to the exit static pressure, which for separated flow is equal to the base pressure (as indicated by the foregoing example). It would be expected, therefore, that any variation in external flow which affects base pressure would also affect the thrust of a nozzle with separated flow.

A measure of the performance of an exhaust nozzle is the ratio of the actual thrust to the ideal thrust corresponding to the operating pressure ratio. The ideal-thrust coefficient for a completely expanded nozzle (exit pressure equal to free-stream static pressure) is presented in figure 9. These values correspond to equation (8) for $\gamma = 1.4$. The ratio of the thrust coefficient calculated for the four nozzles investigated by the pressure-integration technique (eq. (7)) to this ideal thrust coefficient is presented in figure 10 as a function of nozzle pressure ratio and free-stream Mach numbers. Also presented in figure 10 are the theoretical one-dimensional thrust-ratio values for each nozzle.

3142

CP-2

The thrust-ratio data for the conical-element nozzle (fig. 10(a))
agree very well with the one-dimensional theory for nozzle pressure
ratios greater than about 3.0 for all free-stream Mach numbers tested.
Such agreement would be expected since the loss in thrust due to the
radial component of momentum is small for nozzles of small divergence
angles. Below pressure ratios of 3.0, the thrust ratio is affected by
free-stream Mach numbers: At a pressure ratio of 2.0, the thrust ratio
is approximately 0.96 at M_0 of 0.1 compared with 0.90 at M_0 of 2.0.
The increase of thrust ratio over the theoretical one-dimensional value
at the lower Mach numbers and low pressure ratios is due to the favorable
pressure rise in the divergent section resulting from the flow separation
within the nozzle and is evidently related to the variation of model base
pressure with free-stream Mach number.

A nozzle geometrically similar to the conical-element configuration
of the present investigation was tested in quiescent air and the results
are reported in reference 1. The thrust data of reference 1 were ob-
tained by force measurements and therefore include the friction losses
neglected by the pressure-integration technique. If the data of refer-
ence 1 are assumed comparable with the Mach 0.1 data, the difference in
the thrust ratio obtained by the two methods (fig. 10(a)) indicates that
the friction losses are on the order of 3 percent over most of the noz-
zle pressure-ratio range for which both sets of data are available.

The thrust-ratio data for the uniform-exit nozzle (fig. 10(b)) also
indicate good agreement with the theoretical one-dimensional values over
the entire range of pressure ratios investigated, with no appreciable
effect of free-stream Mach numbers. From a thrust standpoint, the
uniform-exit design has no apparent advantage over the conical-element
nozzle; in fact, it may be somewhat less desirable because no favorable
Mach number effects occurred at the low pressure ratios. The friction
losses in this nozzle may also be higher than for the conical-element
nozzle because of the greater over-all length.

The thrust-ratio data for the rapid-divergent nozzle with a design
pressure ratio of 5.7 (fig. 10(c)) fall below the theoretical one-
dimensional values by 2 to 3 percent at pressure ratios above about 5.0.
This loss is a result of the low wall static pressures caused by the
rapid divergence (fig. 7). At low pressure ratios and subsonic Mach
numbers, however, flow separation in the nozzle results in thrust ratios
considerably in excess of theoretical. At a pressure ratio of 2.0, the
computed thrust ratio of 0.98 was higher than for either of the more-
gradual-divergent nozzles (1 and 2). This same effect was present to a
lesser degree at a free-stream Mach number of 1.6. At M_0 of 2.0, this
advantage did not exist; the thrust ratio at a pressure ratio of 2.0 was
approximately the same as for the more-gradual-divergent nozzles.

The other rapid-divergent nozzle (fig. 10(d)) exhibited similar characteristics, with the effects magnified by the fact that the geometry corresponded to a design pressure ratio of 9.1 rather than 5.7. The free-stream Mach number effect at the low pressure ratios was very large for this nozzle, the difference between M_0 of 0.1 and 2.0 amounting to approximately 25 percent of the ideal thrust at a pressure ratio of 2.0. No Mach number effect was observed at pressure ratios greater than about 7.0. In this range the experimental thrust was about 3.5 percent below the theoretical one-dimensional values.

It would appear that the rapid-divergent nozzles might have an over-all thrust advantage over the more-gradual-divergent configurations if a wide range of nozzle pressure ratios are required for operation, providing the low pressure ratios occur only at subsonic flight speeds. The relatively short length of these nozzles would also be advantageous from a weight standpoint and might result in smaller thrust losses due to friction than the more-gradual-divergent designs, thus increasing the relative importance of the rapid-divergent nozzles.

SUMMARY OF RESULTS

An experimental investigation of a series of four convergent-divergent exhaust nozzles was conducted in the Lewis 8- by 6-foot supersonic wind tunnel at free-stream Mach numbers of 0.1, 0.6, 1.6, and 2.0 over a range of nozzle pressure ratios. The thrust characteristics of these nozzles were determined by a pressure-integration technique. The following results were obtained:

1. The thrust characteristics of the gradual-divergent nozzles indicated that the nozzle designed to give uniform parallel flow at the exit had no advantage over the simple geometric design with conical convergent and divergent sections. The rapid-divergent nozzles might be competitive with the more-gradual-divergent nozzles since the relatively short length of these nozzles would be advantageous from a weight standpoint and might result in smaller thrust losses due to friction.

2. The thrust characteristics, with friction losses neglected, were predicted satisfactorily by one-dimensional theory for the nozzles with relatively gradual divergence, except that a conical-element design experienced some gain in thrust as a result of flow separation within the nozzle at low pressure ratios and low free-stream Mach numbers.

3. The thrust for nozzles with rapid divergence was several percentages below the theoretical values except for pressure ratios considerably below the design value. In this range the flow separation within the nozzle increased the thrust appreciably above the theoretical values, with the greatest effect noted for subsonic stream flow.

3142

CP-2 back

4. When separation occurred within a given nozzle, the effect of free-stream Mach number on thrust appeared to be related to the variation of base pressure with free-stream Mach number.

Lewis Flight Propulsion Laboratory
        National Advisory Committee for Aeronautics
            Cleveland, Ohio, December 22, 1953

REFERENCES

1. Krull, H. George, and Steffen, Fred W.: Performance Characteristics of One Convergent and Three Convergent-Divergent Nozzles. NACA RM E52H12, 1952.

2. Hearth, Donald P., and Gorton, Gerald C.: Investigation of Thrust and Drag Characteristics of Plug-Type Exhaust Nozzle. NACA RM E53L16 , 1954.
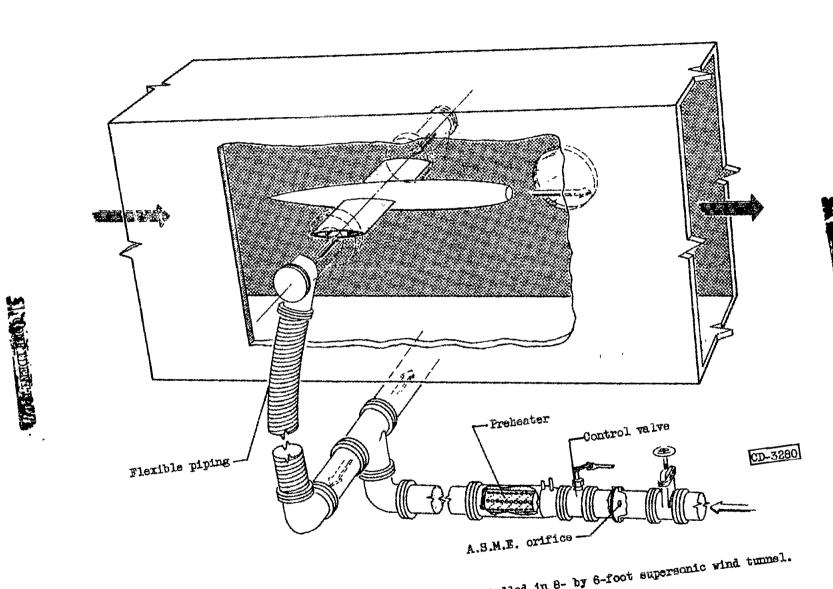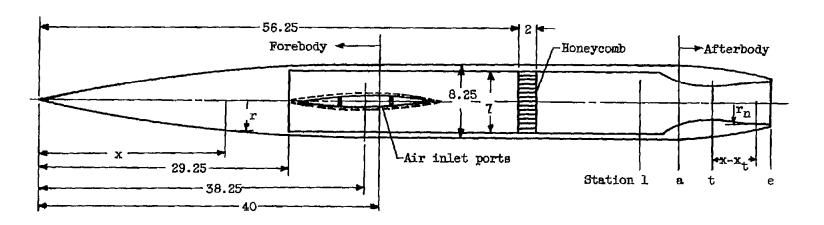
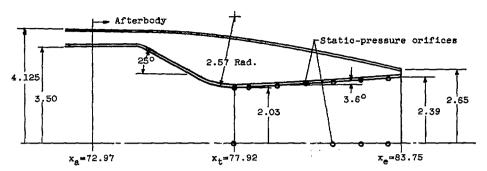Figure 1. - Schematic diagram of jet-exit model installed in 8- by 6-foot supersonic wind tunnel.

Flexible piping

Preheater

Control valve

A.S.M.E. orifice

CD-3280

3142

Forebody

Honeycomb → Afterbody

56.25 — 2

8.25

7

r

r_n

Air inlet ports

x

29.25

38.25

40

$x-x_t$

Station 1   a   t   e

Forebody equation:
$$r = 4.125 - 0.00258(40-x)^2$$

Afterbody equation:
$$r = 4.125 - 0.0127(x-x_a)^2$$

Nozzle	x_a	x_t
1	72.97	77.92
2	74.97	79.47
3	72.97	81.75
4	74.13	81.00

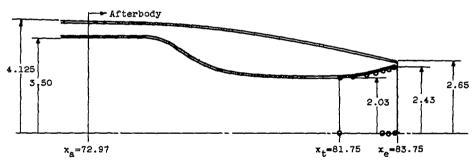| Nozzle coordinates								
Convergent section		Divergent sections						
Nozzle								
2 to 4		2		3		4		
$x-x_t$	r_n	$x-x_t$	r_n	$x-x_t$	r_n	$x-x_t$	r_n	
-6.80	3.50	0	2.03	0	2.03	0	2.03	
-6.50	3.48	.50	2.06	.50	2.06	.50	2.06	
-6.00	3.28	1.00	2.11	1.00	2.15	1.00	2.15	
-5.00	2.62	2.00	2.23	1.50	2.27	1.50	2.27	
-4.00	2.24	3.00	2.33	2.00	2.43	2.00	2.43	
-3.00	2.08	4.00	2.38	----	-----	2.25	2.52	
-2.00	2.035	5.00	2.41	----	-----	2.50	2.62	
-1.00	2.031	6.00	2.43	----	-----	2.75	2.75	
0	2.030	6.28	2.43	----	-----	----	-----	

Figure 2. - Geometric characteristics of jet-exit model.   (All dimensions in inches.)
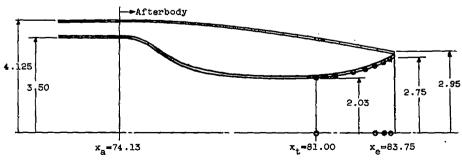
(a) Nozzle 1 (conical element). Design pressure ratio, 5.3.

(b) Nozzle 2 (uniform exit). Design pressure ratio, 5.7.

(c) Nozzle 3 (rapid divergent). Design pressure ratio, 5.7.

(d) Nozzle 4 (rapid divergent). Design pressure ratio, 9.1.

Figure 3. - Sketch of nozzle - afterbody configurations and nozzle pressure instrumentation. (All dimensions in inches.)
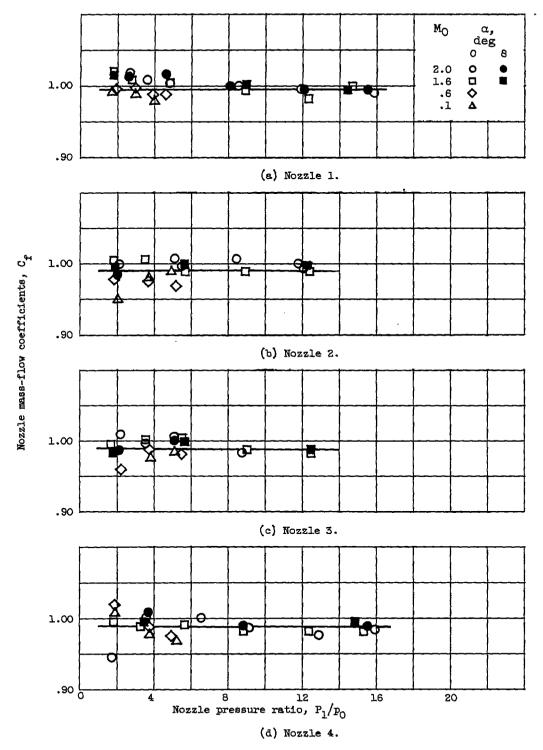
3142

(a) Nozzle 1.

(b) Nozzle 2.

(c) Nozzle 3.

(d) Nozzle 4.

Figure 4. - Nozzle mass-flow coefficients for range of free-stream Mach numbers M_0 at angles of attack α of zero and 8°.

Base
pressure
ratio,
p_b/P_1

Nozzle
pressure
ratio,
P_1/p_0

--- Isentropic one-
dimensional flow

	Base pressure ratio, p_b/P_1	Nozzle pressure ratio, P_1/p_0
σ		1.96
□		2.97
⋈		3.98 4.60

(a) Free-stream Mach number, 0.1.

	Base pressure ratio, p_b/P_1	Nozzle pressure ratio, P_1/p_0
σ		1.94
□		3.00
⋈		3.98 4.62

(b) Free-stream Mach number, 0.6.

Pressure ratio, p/P_1

		1.81 1.86
⋈		2.83 3.63
▽		4.95
		8.98 12.36 14.62

(c) Free-stream Mach number, 1.6.

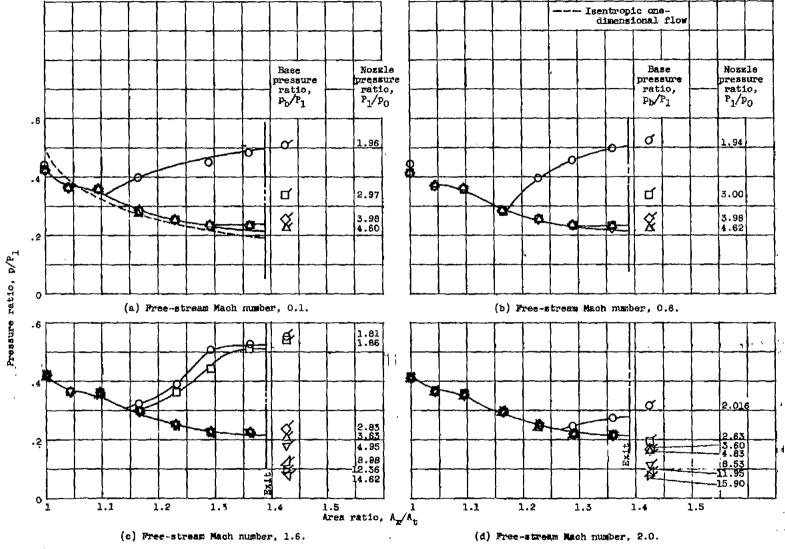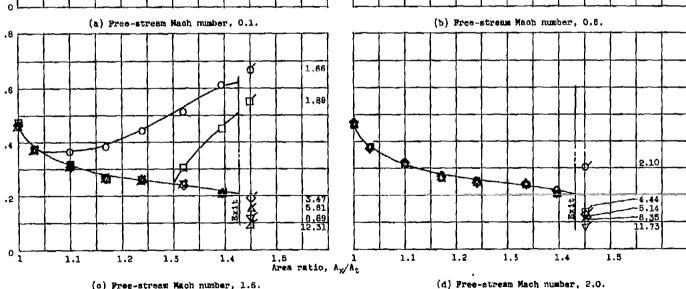|		
σ		2.016
□		2.83
⋈		3.60 4.83
▽		8.53
		11.95 15.90

(d) Free-stream Mach number, 2.0.

Area ratio, A_x/A_t
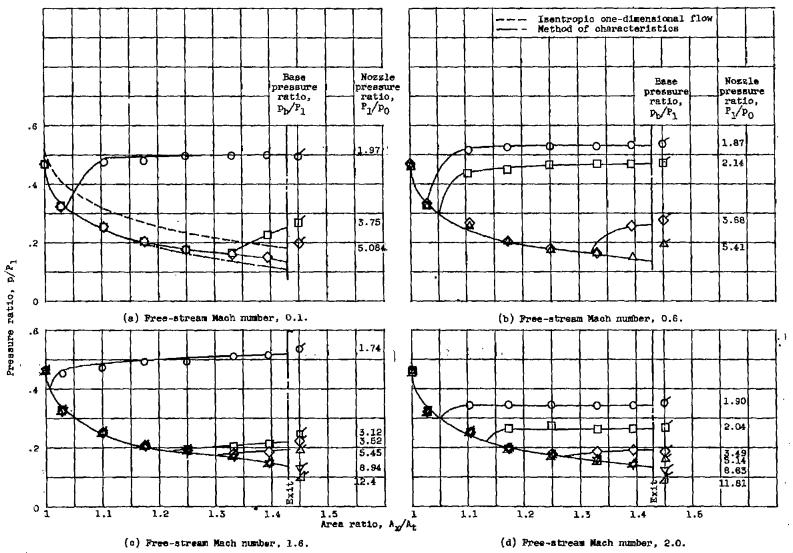
Figure 5. - Nozzle pressure distributions and base pressures for range of pressure ratios and free-stream Mach numbers. Nozzle 1 (conical element). Design pressure ratio, 5.3.

Base pressure ratio, P_b/P_1 | Nozzle pressure ratio, P_1/p_0

1.97

3.75

4.98

(a) Free-stream Mach number, 0.1.

--- Isentropic one-dimensional flow
— Method of characteristics

Base pressure ratio, P_b/P_1 | Nozzle pressure ratio, P_1/p_0

1.90

3.78

5.07

(b) Free-stream Mach number, 0.8.

Pressure ratio, p/P_1

.6

.4

.2

0

.8

.6

.4

.2

0

1.66

1.89

Exit

3.47
5.81
8.89
12.31

(c) Free-stream Mach number, 1.6.

2.10

4.44
6.14
8.35
11.73

Exit

(d) Free-stream Mach number, 2.0.

1   1.1   1.2   1.3   1.4   1.5

Area ratio, A_x/A_t

Figure 6. - Nozzle pressure distributions and base pressures for range of pressure ratios and free-stream Mach numbers. Nozzle 2 (uniform exit). Design pressure ratio, 5.7.

(a) Free-stream Mach number, 0.1.

(b) Free-stream Mach number, 0.6.

(c) Free-stream Mach number, 1.6.

(d) Free-stream Mach number, 2.0.

Figure 7. – Nozzle pressure distributions and base pressures for range of pressure ratios and free-stream Mach numbers. Nozzle 3 (rapid divergent). Design pressure ratio, 5.7.
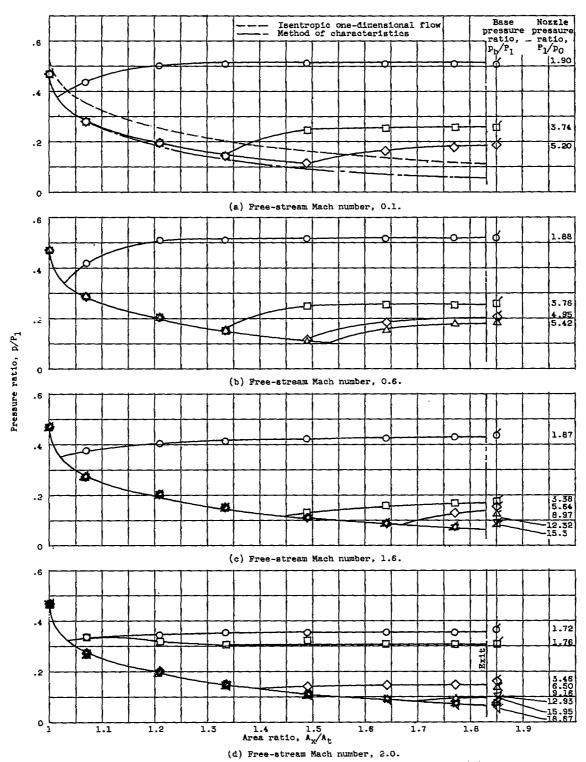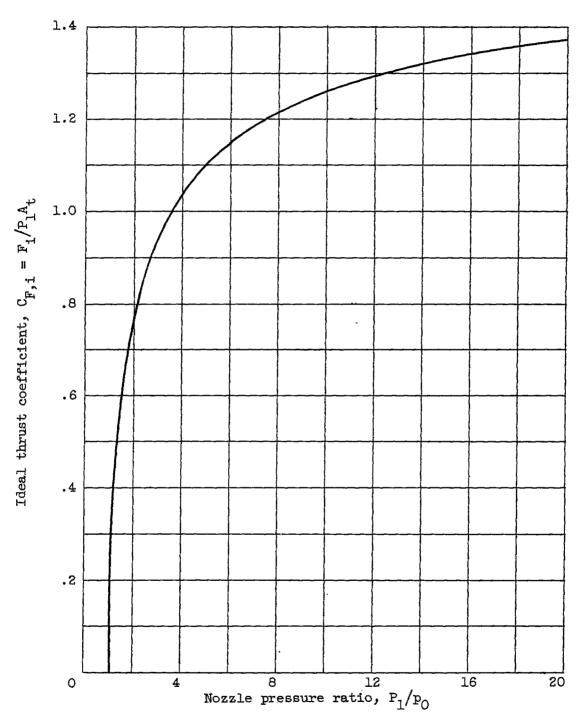
3142

CP-3 back

(a) Free-stream Mach number, 0.1.

(b) Free-stream Mach number, 0.6.

(c) Free-stream Mach number, 1.6.

(d) Free-stream Mach number, 2.0.

Figure 8. - Nozzle pressure distributions and base pressures for range of pressure ratios and free-stream Mach numbers. Nozzle 4 (rapid divergent). Design pressure ratio, 9.1.

Figure 9. - Ideal thrust coefficient for nozzle expanded to free-stream static pressure. Ratio of specific heats, 1.4
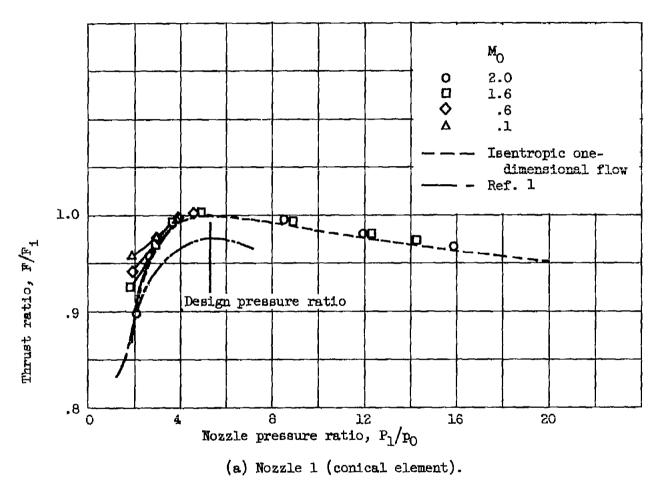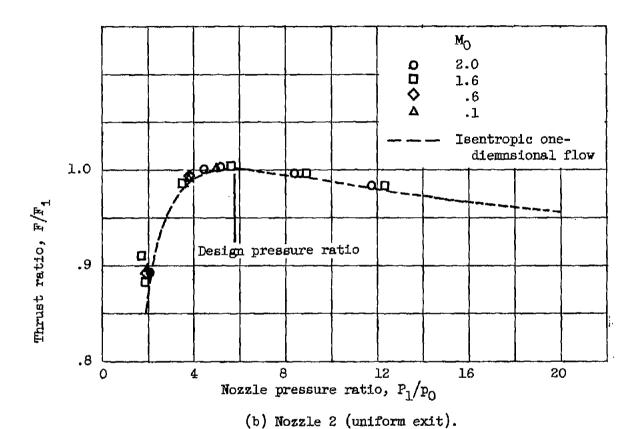
(a) Nozzle 1 (conical element).

Figure 10. - Nozzle thrust-ratio characteristics for range of free-
stream Mach numbers M_0.

(b) Nozzle 2 (uniform exit).

Figure 10. - Continued. Nozzle thrust-ratio characteristics for range of free-stream Mach numbers M_0.
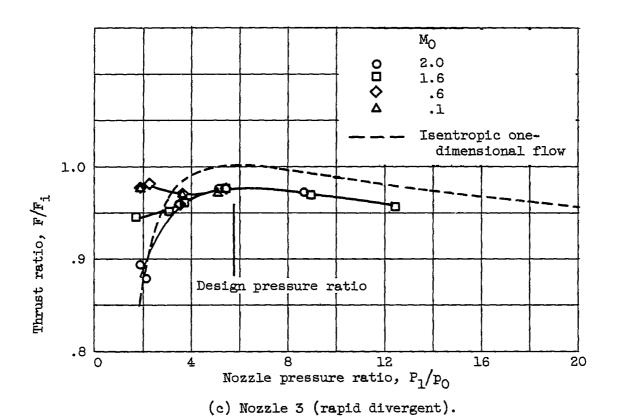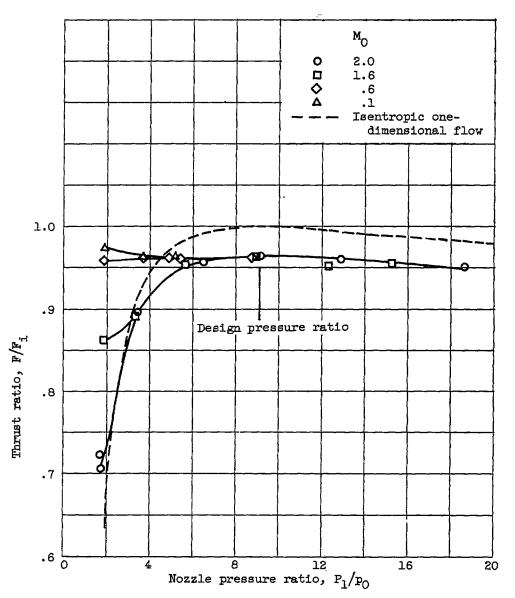
3142

(c) Nozzle 3 (rapid divergent).

Figure 10. - Continued. Nozzle thrust-ratio characteristics
for range of free-stream Mach numbers M_O

(d) Nozzle 4 (rapid divergent).

Figure 10. - Concluded. Nozzle thrust-ratio characteristics
for range of free-stream Mach numbers M_0.